

Supplementary Materials for “Magnus Hall Effect in Two-dimensional Materials”

1. CALCULATION METHODS

The first-principles calculations based on density functional theory (DFT) are performed by using the QUANTUM-ESPRESSO package[1]. Ultrasoft pseudopotentials and general gradient approximation (GGA) according to the Perdew-Burke-Ernzerhof (PBE) functional are used. The energy cutoff of the plane wave (charge density) basis is set to 50 Ry (500 Ry). The DFT Bloch wave functions are projected to maximally localized Wannier functions by Wannier90 code [2, 3]. The Berry curvature is calculated by the WannierTools software package [4]. The spin-orbit coupling is included in all the electronic calculations. The crystal structures are set to make the vertical mirrors or axis be perpendicular to the x direction. All of the band structures are cross-checked by the VASP codes, and the results are consistent with each other.

2. THE BERRY CURVATURE UNDER C_3 SYMMETRY

Every \mathbf{k} point under the C_3 and \mathcal{T} will transform into six points, as shown in Fig. S1. The relationships of velocity and Berry curvature of the six points are listed in Table S1. We can conclude that the C_3 and \mathcal{T} symmetry cannot guarantee the j_y^0 vanishing according to Eq. (2) in the main text.

3. ANTISYMMETRIC CHARACTERISTIC OF TRANSVERSE CURRENT USING GREEN FUNCTION METHOD

We study the transverse current when the vertical mirror or in-plane two-fold symmetries are not perpendicular to the x axis with the non-equilibrium Green’s function method[5, 6]. The effective Hamilton with C_{2v} symmetry reads as:

$$H(\mathbf{k}) = Ak^2 + (Bk^2 + \delta) \sigma_z + v_y k_y \sigma_y + D \sigma_x. \quad (1)$$

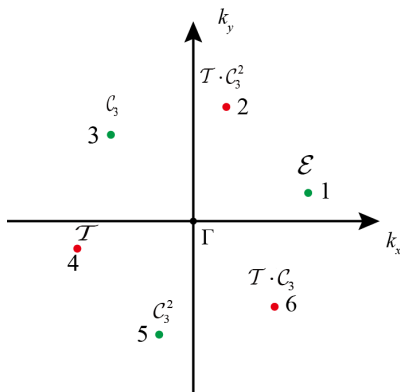


FIG. S1: \mathbf{k} points under the C_{3z} and \mathcal{T} symmetry. The green and red dots stand for the \mathbf{k} points have the opposite Berry curvature value.

TABLE S1: The relationships of velocity and Berry curvature of the six points in Fig. S1. \mathcal{E} means the identity symmetry.

Point	Operation	Velocity	Ω_z
1	\mathcal{E}	(v_x, v_y)	Ω_z
3	C_{3z}	$\left(-\frac{v_x}{2} - \frac{\sqrt{3}v_y}{2}, \frac{\sqrt{3}v_x}{2} - \frac{v_y}{2}\right)$	Ω_z
5	C_{3z}^2	$\left(-\frac{v_x}{2} + \frac{\sqrt{3}v_y}{2}, -\frac{\sqrt{3}v_x}{2} - \frac{v_y}{2}\right)$	Ω_z
2	$\mathcal{T} \cdot C_{3z}^2$	$\left(\frac{v_x}{2} - \frac{\sqrt{3}v_y}{2}, \frac{\sqrt{3}v_x}{2} + \frac{v_y}{2}\right)$	$-\Omega_z$
4	\mathcal{T}	$(-v_x, -v_y)$	$-\Omega_z$
6	$\mathcal{T} \cdot C_{3z}$	$\left(\frac{v_x}{2} + \frac{\sqrt{3}v_y}{2}, -\frac{\sqrt{3}v_x}{2} + \frac{v_y}{2}\right)$	$-\Omega_z$

where $A = 0$, $B = 1$, $\delta = -0.25$, $v_y = 1.0$ and $D = 0.1$. Then, a voltage drop ΔU is added between the two terminals of the system. The sample size is 80×100 , and disorder $w=0.2$.

The calculated G_{yx} of 0° and 180° with the non-equilibrium Green’s function (NEGF) method are shown in Figs. S2 (a) and (b). Because the vertical mirror and in-plane two-fold symmetries are perpendicular to the x axis, only the Magnus Hall part contributes to the transverse current, and G_H are opposite in these two situations. Then, the Hamiltonian in Eq. (1) is rotated counter-clockwise by 45° and $45^\circ + 180^\circ$, respectively. When the sample is rotated 45° , the vertical mirror and in-plane two-fold symmetries are not perpendicular to the x axis, the Magnus Hall signals accompany with trivial transverse signals. However, we found that the G_{yx} shows the asymmetry under 45° and $45^\circ + 180^\circ$, in Figs. S2 (c) and (d). Because G_y^0 remains invariant, while the G_H is reversed. So the total transverse conductance changes from $G_y^0 + G_H$ to $G_y^0 - G_H$, therefore the antisymmetric part of the total transverse current of these two cases correspond to the Magnus Hall current. The calculated results agree with our symmetry analysis.

4. AFFECT ON LONGITUDINAL ACCELERATION OF ELECTRONS

The built-in electric field is very small, and the wave packet momentum \mathbf{k} does not change substantially under the built-in electric field in the MHE theory [7]. This assumption is reasonable, which can be obtained in the following estimation. The electron velocity $v \sim 10^6$ m/s [8] in conventional metals. If the length of the bottom gate $L=100$ nm and $\Delta U = 0.1$ eV, we get

$$\Delta k \approx -\frac{1}{\hbar} \frac{\Delta U}{v_x} \approx 0.015 \text{ \AA}^{-1} \quad (2)$$

according to Eq. 1 of Ref. [7]. Δk is very small relative to the reciprocal lattice (in the order of $2\pi \text{ \AA}^{-1}$). Correspondingly, the electron velocity \mathbf{v} is basically invariant during the Magnus Hall transport. Besides, the nonequilibrium Green’s function method (Landauer-Buttiker simulation) in Ref. [7] and our work do not adopt the assumption that crystal momentum \mathbf{k} and velocity is conserved. However, the results basically match with those using the assumption.

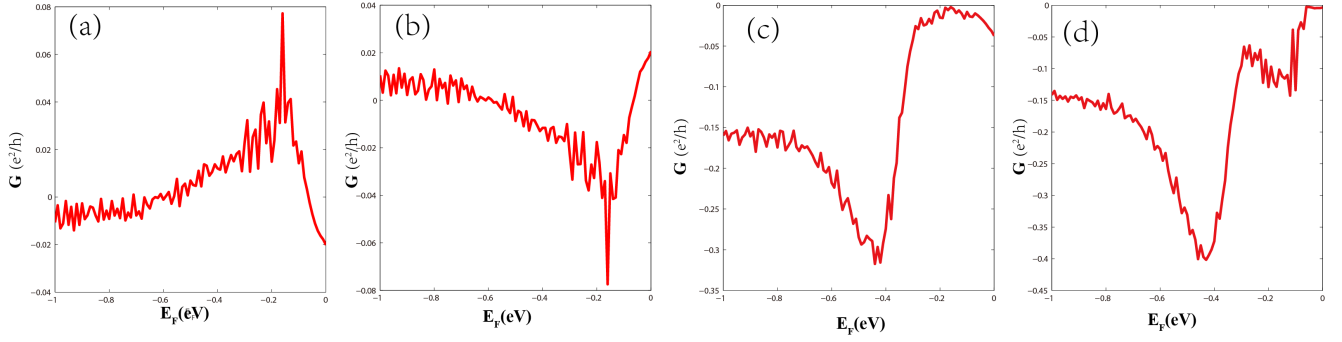


FIG. S2: The transverse conductance when the sample is rotated to (a) 0° , (b) 180° , (c) 45° , and (d) $45^\circ + 180^\circ$. The burr is due to the Fabry-Perot resonance in the sample.

If the assumption that crystal momentum conservation breaks down, we think the Magnus Hall can also exist. Eq. 2 of Ref. [7] will be

$$\Delta y_A = - \int_0^t \frac{\Omega_z(\mathbf{k})}{\hbar} \frac{\partial U}{\partial x} dt = - \int_0^L \frac{\partial k_x}{\partial \varepsilon(\mathbf{k})} \Omega_z(\mathbf{k}) \frac{\partial U}{\partial x} dx \quad (3)$$

where t is the transit time through the electric field region. During this time, crystal moment changes, *i.e.*, is the function of time t . This equation will be very complicated, cannot have an analytical solution. In this case, we have to adopt the nonequilibrium Green's function method to study this, while it is beyond the scope of our study.

-
- [1] P. Giannozzi, S. Baroni, N. Bonini, M. Calandra, R. Car, C. Cavazzoni, D. Ceresoli, G. L. Chiarotti, M. Cococcioni, I. Dabo, A. D. Corso, S. d. Gironcoli, S. Fabris, G. Fratesi, R. Gebauer, U. Gerstmann, C. Gougoussis, A. Kokalj, M. Lazzeri, L. Martin-Samos, N. Marzari, F. Mauri, R. Mazzarello, S. Paolini, A. Pasquarello, L. Paulatto, C. Sbraccia, S. Scandolo, G. Sclauzero, A. P. Seitsonen, A. Smogunov, P. Umari, and R. M. Wentzcovitch, *J. Phys.: Condens. Matter.* **21**, 395502 (2009).
- [2] A. A. Mostofi, J. R. Yates, Y.-S. Lee, I. Souza, D. Vanderbilt, and N. Marzari, *Comput. Phys. Commun.* **178**, 685 (2008).
- [3] A. A. Mostofi, J. R. Yates, G. Pizzi, Y.-S. Lee, I. Souza, D. Vanderbilt, and N. Marzari, *Comput. Phys. Commun.* **185**, 2309 (2014).
- [4] Q. Wu, S. Zhang, H.-F. Song, M. Troyer, and A. A. Soluyanov, *Comput. Phys. Commun.* **224**, 405 (2018).
- [5] Q. Yan, Y.-F. Zhou, and Q.-F. Sun, *Chin. Phys. B.* **29**, 097401 (2020).
- [6] Y.-H. Li, J. Liu, J. Song, H. Jiang, Q.-F. Sun, and X. Xie, *Science China Physics, Mechanics & Astronomy* **61**, 97411 (2018).
- [7] M. Papaj and L. Fu, *Phys. Rev. Lett.* **123**, 216802 (2019).
- [8] D. Gall, *J. Appl. Phys.* **119**, 085101 (2016).